THE PALISADES OF VOGT IN CONGENITAL CORNEAL OPACIFICATION (AN AMERICAN OPHTHALMOLOGICAL SOCIETY THESIS)

By Ken K. Nischal MD and Kira L. Lathrop MAMS

ABSTRACT

Purpose: The purposes of this study are first, to determine if the palisades of Vogt (POV) are present or absent in cases of congenital corneal opacification (CCO) by using spectral domain ocular coherence tomography (SD-OCT), and second, in those cases already undergoing penetrating keratoplasty (PKP), to see whether the absence or presence of POV corresponds to re-epithelialization following transplant.

Methods: This was a retrospective case review of 20 eyes (10 normal, 10 with CCO) evaluated with SD-OCT. The operator was masked to the clinician's assessment of the ocular surface. In those cases where the decision to perform PKP had already been made, the correlation between POV presence or absence and posttransplant graft epithelialization was determined.

Results: All cases were imaged without adverse event. Nine eyes showed some evidence of POV and corresponding vasculature. Eight of 10 affected eyes underwent PKP, and subsequently 7 eyes epithelialized and 2 showed some peripheral neovascularization. The one eye that showed no signs of POV was the one that failed to epithelialize .All control subjects had consistent and regular POV.

Conclusions: Congenital corneal opacification is rare, and this study shows that at least some POV are present in the majority of cases of CCO. However, the palisades may not be entirely normal compared to age-matched controls. When there was absence of POV in a case of CCO, there was immediate and complete failure of epithelialization.

Trans Am Ophthalmol Soc 2016;114:T8[1-20].

INTRODUCTION

Neonatal corneal opacification is rare, with an incidence of 1 in 26,000 to 37,000 live births.[1,2] Recently a novel classification has been proposed whereby conditions causing neonatal corneal opacification have been considered as primary corneal diseases or secondary corneal diseases (Table 1).[3,4] The benefit of such a classification is that it begins to define which cases may benefit from surgery and which are more likely to fail.

TABLE 1. CLASSIFICATION OF NEONATAL CORNEAL OPACIFICATION

PRIMARY (DEVELOPMENTAL ANOMALIES OF CORNEA ONLY)

1. Corneal dystrophies: CHED/PPMD
2. Isolated sclerocornea
3. Corneal structural defects due to dermoids
4. CYP1B1 cytopathy[47]

SECONDARY

1. Kerato-irido-lenticular dysgenesis (KILD)
   - Iridocorneal adhesions only
   - Lens fails to separate from cornea
   - Lens separates but fails to form
   - Lens fails to form
   - Due to PHPV
2. Iridotrabecular dysgenesis
   - Infantile glaucoma
   - Axenfeld-Rieger anomaly/syndrome
   - Aniridia
3. Acquired
   - Metabolic
   - Trauma
   - Infection

CHED, congenital hereditary endothelial dystrophy; PHPV, persistent hyperplastic primary vitreous; PPMD, posterior polymorphous dystrophy.

From the Children's Eye Center, Children's Hospital of Pittsburgh of UPMC (Dr Nischal), the Eye and Ear Institute, UPMC (Dr Nischal, Ms Lathrop), the Department of Ophthalmology, University of Pittsburgh School of Medicine (Dr Nischal, Ms Lathrop), and the Department of Bioengineering, University of Pittsburgh Swanson School of Engineering (Ms Lathrop).

Congenital corneal opacification (CCO) includes all the developmental causes of corneal opacity that are present at birth, which include sclerocornea, Peters' anomaly, corneal dermoids and, only very rarely, corneal dystrophies such as posterior polymorphous dystrophy and congenital hereditary endothelial dystrophy. In this study we examined only children with developmental congenital corneal opacities without corneal dystrophies or dermoids.

Infant corneal transplantation has a high risk of failure, which varies depending on the series quoted.[5-24] Most of these studies have not attempted to classify the nature of the opacity using anterior segment imaging techniques,[25] nor have they correlated it with likelihood of failure other than to establish that keratoplasty with simultaneous lensectomy and vitrectomy tends to result in failure.[5-24] Neither is the nature of the transplant failure categorized, so it is not clear whether retrocorneal membranes, epithelial rejection, endothelial rejection, failure of epithelialization, or a combination of all of these have contributed to the failure.

Lamellar keratoplasty or penetrating keratoplasty (PKP) provides a temporary replacement of the host's corneal epithelium, but in order for the epithelium of the donor cornea to be replenished adequately, the host's limbal architecture must be intact and contain normally functioning limbal stem cells.[26] Limbal stem cells are slowly recycling cells that divide and subsequently differentiate into transient amplifying cells, which then become corneal or conjunctival epithelial cells.[26] Evaluation of limbal stem cell function at present is done purely indirectly by looking at cytokeratin staining of the corneal epithelium using impression cytology.[26]

Growth of conjunctival epithelium over the cornea is prevented by the presence of an intact limbal epithelium.[27-30] The limbal epithelium is 7 to 10 layers thick and arises in a loose connective tissue intermixed with its transient amplifying cells in an anatomically distinct structure called the palisades of Vogt (POV), where the basal stem cells are nurtured by this special highly vascularized and innervated microenvironment.[29]

There is evidence that the presence of a specialized niche (POV) is indicative of normal-functioning limbal stem cells. This evidence comes from indirect findings, such as degradation of palisade architecture with progression of the well-established limbal stem cell deficiency (LSCD) seen in aniridia due to PAX6 mutations[31] and the loss of POV in areas known previously to have had palisade architecture (eg, after alkali injury), where there is conjunctivalization of the adjacent cornea and presence of conjunctival epithelium and goblet cells.[26] Complete replacement of the corneal epithelium may take up to a year,[27,31] and although the basal layers of the cornea may have some reserve to replenish corneal epithelium,[26,27] this is not sustainable without intact limbal stem cells.

Limbal stem cell deficiency may be primary (seen in aniridia due to PAX6 mutations, ectodermal dysplasia, keratitis secondary to multiple endocrine adenomatosis, autosomal dominant keratits[30,32-34]) or acquired (eg, alkali injury, Stevens-Johnson syndrome). The incidence or association of LSCD in developmental neonatal corneal opacities is not known. A Medline search using the search terms *LSCD* and *sclerocornea* or *Peters' anomaly* or *anterior segment dysgenesis* failed to reveal any references.

In an extensive review of the literature examining the genetic causes of CCO, the term *sclerocornea* was found to be used interchangeably with complete corneal opacification.[35] The novel classification mentioned above (see Table 1)[3,4] describes these phenotypes as being secondary to another intraocular disease, which has resulted in total corneal opacification. There is no published data as to whether these cases have normal POV or functioning limbal stem cells.

Clinical indicators of LSCD are conjunctivalization of the cornea, neovascularization, and chronic inflammation. The corneal epithelium develops a dull and irregular light reflex on slit-lamp biomicroscopy with variable loss of transparency and variable thickness. Complications such as recurrent or persistent epithelial corneal defects, scarring, calcification, superficial neovascularization, and sometimes perforation may be seen.[26] Limbal stem cell deficiency may be localized or diffuse, and diagnosis is complicated because many of these signs may also be seen in chronic inflammation from other causes and are therefore not pathognomonic of LSCD.

Detecting limbal stem cell dysfunction has hitherto relied on clinical signs and impression cytology.[26] Evaluation with impression cytology provides indirect evaluation of LSCD by detection of characteristic cytokeratins that are expressed preferentially on the uppermost layer(s) of either the corneal or conjunctival epithelium.[36-39] Cytokeratins K12 and K3 are expressed by corneal epithelium, whereas K19 and MUC1 are expressed in conjunctival epithelium. Traditionally, periodic acid–Schiff staining has also been performed on impression cytology specimens to look for goblet cells, which should be seen only in conjunctival epithelium. Sample acquisition utilizes a membrane that has to be applied to the ocular surface and then fixed in appropriate medium for cytologic evaluation.[36-39] Most children are not able to cooperate safely enough to have such a test done in the clinic. More important, impression cytology may be equivocal in its findings, and giving a child an anesthetic to perform the test may not be justified.

While clinical confocal microscopy can be used to assess the POV, this is a contact method during which the patient is examined while sitting upright. Reports using confocal microscopy describe the presence of three particular features in vivo to demonstrate morphologically intact POV: epithelial basal cells with dark cytoplasm and reflective cell borders; prominent palisade ridge features; and a circular and/or oval-shaped focal stromal projection.[30,40-42] The level of cooperation needed for a child to sit upright at the instrument and allow a contact examination on the cornea excludes this technique for the pediatric population.

Lathrop and associates[43] have shown that spectral domain ocular coherence tomography (SD-OCT) can be used to image the POV, and that the regions evaluated for putative POV co-localized to basal membranes that stained positive for collagen Type VII. Collagen Type VII is known to specifically label the limbal basal membranes. This technique can be applied clinically with a commercially available SD-OCT for noncontact imaging of the POV.

Our primary hypothesis is that children with primary CCO may still have POV as detected with SD-OCT and that CCO does not necessarily preclude functioning limbal stem cells. Our secondary hypothesis is that determination of the presence of POV by OCT may correlate with postkeratoplasty epithelialization.

METHODS

Institutional review board approval was granted from the University of Pittsburgh IRB, and a retrospective case note review was performed on children presenting to the Department of Pediatric Ophthalmology at Children's Hospital of Pittsburgh of UPMC who were diagnosed as having congenital corneal opacity. A summary of the cases is presented in Tables 2 through 5. Where available, molecular test results were recorded from the case note review.

Ten eyes of age-matched controls were also examined prospectively. The details of the controls are given in Table 6.

All OCT images were acquired using the handheld OCT system (Envisu Spectral Domain Ophthalmic Imaging Systems, Bioptigen, Research Triangle Park, North Carolina) in an adjustable custom mount that accommodates supine patients. Eighteen children were imaged in the surgical suite while under anesthesia, and two were imaged in the clinic with the patients awake. The images were acquired using the rectangular volume setting with an area of 4×4 mm. The resolution in tissue was 2.4 μm with a scan depth of 2.5 mm. Once acquired, images were reconstructed and processed using Fiji (ImageJ software developed by Wayne Rasband, National Institutes of Health, Bethesda, Maryland; http://rsb.info.nih.gov/ij/index.html) software and custom-built macros. Once this was done, the best static scan was taken for each plane (x, y, z) and a composite of the three planes was made for evaluation. Figure 1 shows what each plane represents. The three planes are shown here as static images, but videos of all the stacks of images were reviewed, as this gives a better understanding of the information available, much like the fact that dynamic ultrasound B-scan is preferable to assess the presence of a retinal detachment but often static scans are used to demonstrate the presence or absence of a retinal detachment.

Palisade volumes acquired at upright OCT systems often display significant signal falloff because it is difficult to present the limbus perpendicular to the instrument (Figure 2, far left). The fluidity of the handheld OCT system facilitates pediatric and intrasurgical imaging, but the volumes necessary for palisade imaging reflect motion artifact, which confounds registration and segmentation of the volumes (Figure 2, second from left). In addition, volume imaging with a handheld device can be very slow because of difficulty locating and holding a position by hand and because repeated imaging of the same area becomes very subjective. To overcome this, we developed a mount for the handheld OCT (Figure 2, far right), which stabilized volume acquisition and allowed us to avoid including the heartbeat, respiration, and motion artifact of the examiner in the image volumes (Figure 2, second from right). In addition, the mount allowed the OCT to be angled so that the limbus was presented perpendicular to the tissue, which moderated signal falloff. With use of the mount, the only remaining motion artifact seen in the reconstructed sagittal image (Figure 2, second from right) is due to the heartbeat and respiration of the subject, which can be corrected with volume registration.

CASE REPORTS

Case 1 (Figure 3)

A 5-year-old Asian girl, adopted soon after birth, was referred to our department with a history of bilateral congenital corneal opacities and nystagmus. Penetrating keratoplasty had been deferred at several centers on the basis that clinically she had evidence of LSCD. Her best-corrected visual acuity was counting fingers at 2 feet OD and counting fingers at 3 feet OS. Corneal haze precluded retinoscopy, funduscopy, and anterior segment evaluation bilaterally. Examination under anesthesia (EUA) revealed intraocular pressure (IOP) of 8 mm Hg bilaterally. Both corneas appeared flat with thickened nodular opacification in the center with scarring and 360° vascularization. There was scleralization of the cornea in the superior and inferior half in both eyes with indistinct limbus. Ultrasound biomicroscopy showed bilateral normal anterior segment with clear lenses. Axial length was 22.9 mm in the right eye and 22.3 mm in the left eye. On the basis of these findings, a clinical diagnosis of severe cornea plana with questionable limbal stem cell function was made. Impression cytology was performed in both eyes but reported as equivocal due to insufficient sampling.

After much counseling the patient underwent PKP in the right eye followed by the left eye 8 months later. In both eyes there was immediate and normal graft epithelialization. Both grafts suffered endothelial graft rejection (right ×1 and left ×2). At the last follow-up, 18 months after PKP in the left eye, unaided visual acuity at distance was 20/600 OD and 20/400 OS. With both eyes open, the patient saw 20/200 at near with +14.00 D lenses. Slit-lamp examination of the right eye showed some haze in the periphery with growth of some new vessels, but centrally the cornea was reasonably clear. In the left eye, there was mild neovascularization with evidence of endothelial decompensation. A retrocorneal membrane was seen during OCT of the left eye. Fundus examination revealed healthy optic discs with a cup-disc ratio of 0.3 and normal macula in both eyes. The epithelium was intact and did not stain in either eye.

Histopathology of the right corneal button showed keratinization of the corneal epithelium, calcific band keratopathy involving a fragmented Bowman's layer, extensive vascularization of the stroma with chronic inflammation, and extensive scarring/condensation of the anterior stroma. Histopathology of the left eye showed keratinization of the corneal epithelium, extensive central stromal scarring and thinning with near-complete absence of Bowman's layer, calcific band keratopathy, and subepithelial fibrovascular pannus and vascularization of the corneal stroma with chronic inflammation.

TABLE 2. DEMOGRAPHICS AND CLINICAL FEATURES OF CASES 1 THROUGH 5

CASE	AGE	SEX	CLINICAL DIAGNOSIS	PREVIOUS SURGERIES BEFORE PKP	VISUAL ACUITY AT PRESENTATION		CORNEAL OPACITY	VASCULARIZATION	CONJUNCTIVALIZATION	NORMAL PATIENT	
					OD	OS				AGE	SEX
1	5 yr	F	Cornea plana? OU: LSCD	None	CF 2 ft	CF 3ft	OU+	OU+	OU+	4 yr	F
2	1 mo	M	OD: ASDA with cataract	None	Blinked to light		OD+	None	None	1 mo	M
3	8 yr	F	OD: Phthisis OS: Corneal opacity s/p failed corneal graft with endothelial thickening for congenital corneal opacity	OU: PKP, retinal detachment repair, lensectomy and glaucoma sx with drainage implants	NLP (phthisis)	LP	OS+	None	None	6 yr 7 mo	F
4	5 days	F	OU: ASDA and microcornea OD: Iridocorneal adhesion OS: Keratolenticular adhesion with cataract	None	Blinked to light		OU	OU	Scleralization + OD>OS	1 mo	M
5	13 mo	M	OU: Corneal opacity, congenital glaucoma	OD: Cyclophotocoagulation OS: Trabeculectomy	NA	NA	OD: Diffuse corneal opacity OS: Central opacity with iridocorneal adhesions	Mild	OD: (360° pannus) stops at demarcation line	15 mo	M

ASDA, anterior segment developmental anomaly; CF, counting fingers; LSCD, limbal stem cell deficiency; LP, light perception; NA, not able to do; NLP, no light perception; PKP, penetrating keratoplasty; s/p, status post; sx, surgery.

TABLE 3. OCT FINDINGS OF CASES 1 THROUGH 5

CASE	OCT	POSTERIOR SEGMENT	FLASH VEP	SURGERY PERFORMED	STATUS OF GRAFT AT LAST FOLLOW-UP	STATE OF EPITHELIUM	COMPLICATIONS	BCVA AT LAST FOLLOW-UP		LENGTH OF FOLLOW-UP
								OD	OS	
1	z plane: ridges seen but not regular or uniform x plane: blood vessel seen but not ridges y plane: multiple ridges and blood vessels seen	WNL on USS preop, clinically, postop	OS>OD	OU: PKP	Clear cornea centrally, hazy in periphery with mild new vessels	Epithelialized with no staining at last follow-up	OD: lens endothelial touch	20/600	20/400	18 mo
2	z plane: ridges seen but not regular or uniform x plane: blood vessel seen but not ridges y plane: ridges and blood vessels seen	WNL	WNL	PKP, LS, AV	Haze but mild	Epithelialized with no staining	Glaucoma; needed cyclodiode laser	FF	FF	10 mo
3	z plane: some ridges seen but really not uniform/regular x plane: blood vessels seen y plane: blood vessels and ridges seen	Thickened retinochoroidal layer	WNL	OS: PKP with membrane peeling and vitrectomy	Haze	Epithelialized with stippled staining	Tractional RD needed membranectomy and vitrectomy.	NLP	HM	14 mo
4	Left eye, z plane: ridges seen but not regular or uniform; x plane: blood vessel seen but not ridges; y plane: multiple ridges and blood vessels seen Right eye, z plane: regular and uniform ridges seen; x plane: blood vessels and ridges seen; y plane: blood vessels and ridges seen	OD: WNL OS: abnormal optic nerve with temporal retinal coloboma	WNL	OD: PKP OS:PKP, LS, VIT	OD: clear OS: hazy with deep stromal vascularization	OU: epithelialized with no staining	None	FF (able to pick up objects)	FF (to light only)	13 mo
5	z plane: regular and uniform ridges seen x plane: ridges and blood vessels seen y plane: ridges and blood vessels seen	WNL	WNL	OD: PKP, LS, VIT OS: optical iridectomy	Hazy with clear zones in periphery, better than previous visit	Epithelialized partially with 120° of peripheral NV with haze and opacity	OD: glaucoma; needed cyclodiode laser and Ahmed glaucoma implant OS: cataract needed lensectomy	FF	FF	12 mo

AV, anterior vitrectomy; FF, fix and follows object/light; HM, hand motions; LS, lensectomy; NLP, no light perception; NV, neovascularization; OCT, optical coherence tomography; PKP, penetrating keratoplasty; RD, retinal detachment; USS, ultrasound B-scan; VEP, visual evoked potential; VIT, complete vitrectomy; WNL, within normal limits.

TABLE 4. DEMOGRAPHICS AND CLINICAL FEATURES OF CASES 6 THROUGH 10

CASE	AGE	SEX	CLINICAL DIAGNOSIS	PREVIOUS SURGERIES BEFORE PKP	VISUAL ACUITY AT PRESENTATION		CORNEAL OPACITY	VASCULARIZATION	CONJUNCTIVALIZATION	NORMAL PATIENTS	
					OD	OS				AGE	SEX
6	3 yr	F	OU: congenital glaucoma, aniridia, microcornea, pachymetry OD: 733 µm OS: 1102 µm	OU: trabeculectomy with mitomycin-C, cyclophotocoagulation OD: lensectomy	Blinked to light	OS>OS	None	None	None	3 yr	M
7	12 mo	M	OU: CHED?, PPMD?, X-linked endothelial corneal dystrophy	None	CSM	CSM	OU: stromal edema with endothelial changes	None	None	14 mo	M
8	2 yr	F	OU: glaucoma OS: corneal opacity	OU: goniotomy and Ahmed glaucoma implant	CSM, fixates and follows 3-inch sticker at 1 meter	UATP: No fixation	OD: localized corneal opacity near tip of Ahmed tube OS: diffuse corneal opacity	OS : conjunctivalization stops abruptly at a demarcation line	None	2 yr	M
9	14 yr	F	OU: cloudy cornea Congenital glaucoma	Trabeculectomies, repair of intrastromal bleb	20/300	20/200	OU: central opacity OD>OS, shallow AC, cornea plana OD: microphthalmic	None	OU	15 yr	M
10	4 yr	M	OU: Axenfeld-Rieger syndrome, glaucoma, and s/p glaucoma implants OS: PKP (elsewhere)	OD: drainage tube shortening and flushing, lysis, division of posterior pigment epithelium attachments to the anterior capsule and broad iridectomy OD: LS (elsewhere)	CF 3ft (-4.74 D)	LP (4.50 D)	OD: superotemporal with tube-cornea touch OS: opacity secondary to failed graft	None	None	6 yr 7 mo	F

AC, anterior chamber; CF, counting fingers; CHED, congenital hereditary endothelial dystrophy; CSM, central, steady, maintain fixation; LP, light perception; LS, lensectomy; PKP, penetrating keratoplasty; PPMD, posterior polymorphous dystrophy; s/p, status post; UATP, unable to perform;

TABLE 5. OCT FINDINGS OF CASES 6 THROUGHT 10

CASE	OCT	POSTERIOR SEGMENT	FLASH VEP	SURGERY PERFORMED	STATUS OF THE GRAFT AT LAST FOLLOW-UP	STATE OF EPITHELIUM	COMPLICATIONS	BCVA AT LAST FOLLOW-UP		LENGTH OF FOLLOW-UP
								OD	OS	
6	No ridges or blood vessels seen in any of the planes or on the video stack	Dysplastic and cupped optic nerve with a dysplastic fovea	WNL	OD: PKP OS: PKP, LS, AV	OD: cornea hazy with scarring and vascularization OS: phthisis	Poor epithelialization with keratinization and vessels	OD: postop endophthalmitis OS: exposure keratopathy	NA	Blinked to light	10 mo after right PKP (age 2 yr)
7	z plane: ridges seen, regular but not uniform x plane: ridges and blood vessels seen z- plane: ridges and blood vessels seen	WNL	WNL	None	NA	No PKP performed	NA	NA	NA	23 mo (no surgery)
8	z plane: ridges seen, uniform but not regular x plane: ridges and blood vessels seen y plane: blood vessels and ridges seen	WNL	WNL	OD: Flushing and trimming of drainage tube OS: PKP, repeated PKP, LS, AV	1st graft OS: hazy s/p corneal ulcer 2nd graft OS: epithelial defect centrally with haze	Epithelialized with no new vessels	2nd graft OS: epithelial defect adjacent to donor-host junction step	20/100 with both eyes open		4 mo (after 2nd PKP in OS)
9	z plane: ridges regular but not uniform x plane: blood vessels seen y plane: blood vessels seen	OD: C-D 0.5 with loss of temporal NRR OS: WNL	NA	NA-	NA	No PKP performed	NA	NA	NA	NA
10	z plane: ridges seen but not uniform x plane: ridges seen but blood vessels, though seen, sparse y plane: blood vessels seen	WNL (USS)	Latency OU: WNL amplitude OD: normal OS: reduced	OD: PKP,VIT, membranectomy regraft OS: PKP, LS, VIT	OD: some haze OS: phthisis	Epithelialized but haze secondary to early RCM	OD: RD	20/400 (OD: near vision)	OS: LP	9 mo (after OD PKP)

AV, anterior vitrectomy; BCVA, best-corrected visual acuity; C-D, cup-disc ratio; LS, lensectomy; LP, light perception; NA, not applicable; NRR, neuroretinal rim; OCT, optical coherence tomography; PKP, penetrating keratoplasty; RCM, retrocorneal membrane; RD, retinal detachment; s/p, status post; USS, ultrasound B-scan; VEP, visual evoked potential; VIT, complete vitrectomy; WNL, within normal limits.

TABLE 6. DEMOGRAPHICS AND OCT FEATURES OF NORMAL CONTROLS*

CONTROL	CONTROL AGE	MATCH WITH STUDY CASE	PATIENT AGE	SEX	DIAGNOSIS	OCT FEATURES
1	3 yr 5mo	Case 1	5 yr	F	Clinically normal except cataract lens extraction OD	Ridges seen as regular, consistent with blood vessels at base of ridges
2	1 mo (35 days)	Case 2	1 mo (42 days)	M	Clinically normal except cataract lens extraction OU	Ridges seen but less consistent and variable regularity of visible blood vessels at base of ridges
3	6 yr 7 mo	Case 3	8 yr	F	Clinically normal except undergoing strabismus surgery	Ridges seen as regular, consistent with blood vessels at base of ridges
4	1 mo (35 days)	Case 4	1 mo (44 days)	M	Clinically normal except cataract lens extraction OU	Ridges seen but less consistent and variable regularity of visible blood vessels at base of ridges
5	14 mo	Case 5	13 mo	M	Clinically normal, undergoing suture removal in other eye	Ridges seen as regular, consistent with blood vessels at base of ridges
6	3 yr 5 mo	Case 6	4 yr	M	Clinically normal except cataract lens extraction OU	Ridges seen as regular, consistent with blood vessels at base of ridges
7	14 mo	Case 7	14 mo	M	Clinically normal except cataract lens extraction OU	Ridges seen but less consistent and variable regularity of visible blood vessels at base of ridges
8	22 mo	Case 8	2 yr	M	Clinically normal, undergoing probe and irrigation	Ridges seen as regular, consistent with blood vessels at base of ridges
9	14 yr 5 mo	Case 9	14 yr	M	Clinically normal, had been glaucoma suspect who would not allow exam in clinic	Ridges seen as regular, consistent with blood vessels at base of ridges
10	6 yr 7 mo	Case 10	4 yr	F	Clinically normal except undergoing strabismus surgery	Ridges seen as regular, consistent with blood vessels at base of ridges

OCT, optical coherence tomography.
*It is noteworthy that eyes under the age of 18 months displayed the least consistent ridges on the z-plane view and variable blood vessels on the x-plane view (see control figures for cases 2, 4, and 7: note case 7 control is 14 months old and cases 2 and 4 controls are 1 month old). The older the control, the more consistent the ridges and the blood vessels. See Figures 3, 4, and 5 also.

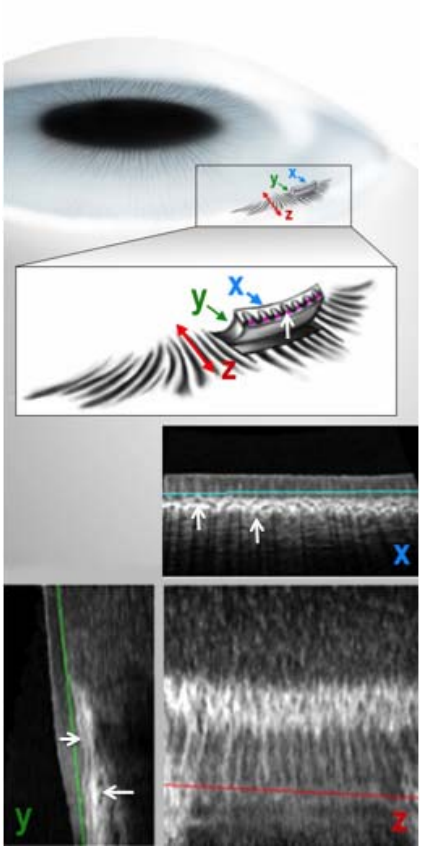

FIGURE 1

Upper half, schematic of three planes. In enface z-plane image the palisade ridges are seen like striations. In x-plane image the ridges with blood vessels (vertical white arrow pointing to pink dots representing the blood vessels) are seen at the base. In y-plane image the blood vessels are seen as circular black spaces, and in x-plane image they appear as long black strings, only part of which are seen. Lower half, SD-OCT scan from a normal control. Palisades of Vogt in z-plane image are shown as ridges. In plane y on dynamic video stacks, scan shows either no ridge or ridge as the scan plane moves through the palisades circumferentially; two prominent dark stringlike structures (horizontal white arrows) are the blood vessels at the base of the palisades. The same blood vessels are seen as circular black spaces at the base of the palisade ridge in x plane (vertical white arrows). Note that in z plane the ridges in normals should be regular and consistent; in x plane the ridges are again regular and consistent but the blood vessels are also seen at the bases and some are deeper. In y plane the dynamic evaluation is more important, much like the evaluation of a retinal detachment on B-scan gives more information than a static B-scan of the same retinal detachment.

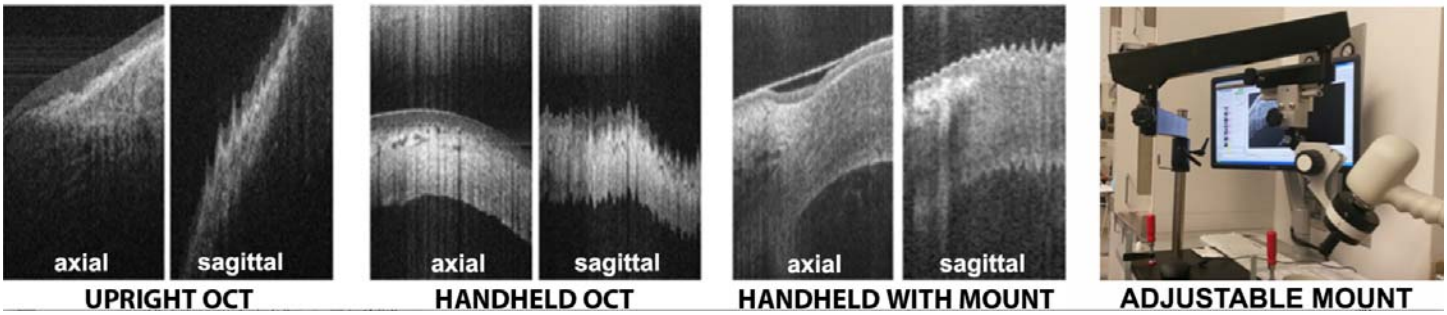

FIGURE 2

Composite of SD-OCT images depicting the movement artifacts induced with the upright OCT (extreme left), handheld OCT (second from left), and handheld OCT with the mount (second from right). The mount (extreme right) is a mechanical arm developed to stabilize and improve image acquisition. Palisade volumes acquired at upright OCT systems often display significant signal falloff because it is difficult to present the limbus perpendicular to the instrument. The fluidity of the handheld OCT facilitates pediatric and intrasurgical imaging, but the volumes necessary for palisade imaging reflect motion artifact, which confounds registration and segmentation of the volumes. Also, volume imaging with a handheld device can be very slow because of difficulty locating and holding a position by hand, and repeated imaging of the same area becomes very subjective. To overcome this we developed a mount for the handheld OCT (extreme right) that stabilized volume acquisition and allowed us to avoid including the heartbeat, respiration, and motion artifact of the examiner in the image volumes (second from right). The mount allowed the OCT to be angled so that the limbus was presented perpendicular to the tissue, which moderated signal falloff.

Case 2 (Figure 3)

An otherwise healthy 5-week-old baby boy from Qatar, born of consanguineous parents, was referred for evaluation of congenital corneal opacity in the right eye. There was no significant family history for ocular or systemic diseases. On visual acuity testing the child blinked to light. At EUA, horizontal corneal diameter (HCD) was 8 mm in the right eye and 11 mm in the left. The left eye was completely normal. In the right eye there was scleralization superiorly of the cornea with an avascular white opacity obstructing the visual axis. A high-frequency ultrasound showed iridocorneal adhesions with a cataract present. The posterior segment was normal on B-scan. Intraocular pressure was normal digitally. On the basis of these findings, a clinical diagnosis of CCO secondary to iridocorneal adhesion with cataract was made, and PKP was performed in the right eye. Flash visual evoked potential (VEP) was within normal range for age in each eye. The OCT volumes were acquired in the surgical suite just prior to PKP with lensectomy and vitrectomy in the right eye.

The patient developed a retrocorneal membrane, which was surgically excised. Ten months after PKP the child was able to fix and follow the light. The right eye was quiet with corneal haze at the endothelial level. There was no evidence of LSCD in the form of epithelial defect, corneal vascularization, or conjunctivalization.

Histology of the corneal button showed keratinization of corneal epithelium, mild vascularization, and chronic keratitis of corneal stroma with central absence of Descemet's membrane and corneal endothelial cells. There was also evidence of adherent pigmented epithelium to one edge of corneal stroma consistent with the diagnosis of iridocorneal adhesion. Bowman's membrane was intact across the central portion of the specimen but did not extend to the peripheral edge. The posterior quarter of the stroma showed decreased lamination and subtle increase in new collagen. Periodic acid–Schiff stain was negative for fungal elements and confirmed the central absence of Descemet's membrane.

Case 3 (Figure 3)

An 8-year-old girl was referred to our department with a history of congenital corneal clouding, glaucoma, and iris abnormalities. The right eye had had two failed retinal detachment repair attempts and three failed corneal transplant attempts, leaving the eye phthisical. In the left eye there was failed corneal graft with endothelial thickening. She had undergone placement of a glaucoma drainage device in both eyes 7 years previously.

The patient had a visual acuity of no light perception OD and light perception OS. At EUA, the IOP was 12 mm Hg in the left eye and less than 5 mm Hg in the right eye. The HCD was 14 mm in the left eye. The axial length was 19.39 mm and pachymetry 997 μm centrally in the left eye. In the left eye there was failed corneal graft with endothelial thickening. There was some band-shaped keratopathy over the corneal transplant on the left side. There was no view of the fundus in either eye. Ultrasound biomicroscopy confirmed that the eyes were aphakic. B-scan revealed a normal posterior segment in the left eye.

The patient was followed up regularly for a year with flash VEP and flash electroretinogram, both of which showed a reduction in amplitude in the left eye. Her IOP was 14 mm Hg at this visit. A PKP with membrane peeling and vitrectomy was performed. She required repair of traction retinal detachment and subsequent membranectomy and vitrectomy with silicone oil. Fourteen months after the corneal transplant, her visual acuity was hand movements OS with a hazy cornea. There was silicone oil up against the graft with a localized area of endothelial decompensation. The epithelium did not take up stain other than in this area, where the stain was punctate.

Histology of the corneal button showed keratinization of the corneal epithelium, calcific band keratopathy, subepithelial fibrovascular pannus, and retrocorneal fibrosis that was negative for elastin staining. Both the Verhoeff–Van Gieson and elastin trichrome stains were negative for elastin fibrils. Periodic acid–Schiff highlighted Descemet's membrane adherent to retrocorneal fibrotic tissue.

Case 4 (Figure 3)

A 5-day-old baby girl with bilateral CCO was referred for further evaluation and possible treatment. Her father had a left eye iris coloboma and scoliosis. On examination, the child blinked to light. Horizontal corneal diameter was 6.5 mm in the right eye and 5 mm in the left eye. The cornea showed scleralization with 360° vascularization in the right eye. Scleralization and vascularization were mostly in the superior half in the left eye. On B-scan the posterior segment was normal in both eyes. Ultrasound biomicroscopy clearly showed iridocorneal adhesions with a shallow anterior chamber in the right eye. In the left eye there was a keratolenticular adhesion with a very large lens, which had cataractous changes at the point of keratolenticular adhesion.

Flash VEP was within age-matched normal limits in both eyes. The patient underwent PKP and lensectomy with vitrectomy in the left eye. Postoperative fundus examination of the left eye revealed an abnormal optic nerve with temporal atypical retinal coloboma. Her postoperative course was complicated by a retrocorneal membrane formation. She developed rejection of the corneal graft at the endothelial level with deep new vessels but with complete epithelialization. Six months after the left eye corneal transplant, she underwent PKP in the right eye. Postoperative fundus examination of the right eye was normal. At the last follow-up, 13 months after the right corneal transplant, she was able to fix and follow the light and able to pick up objects. Her graft was clear in the right eye with complete epithelialization without vascularization.

Histology in the left eye showed epidermalization of the corneal epithelium, stromal disorganization with extensive vascularization, absence of Bowman's layer, Descemet's membrane, and endothelium. The right eye showed keratinization of the corneal epithelium, absence of Bowman's layer, Descemet's membrane, and endothelium with stromal disorganization with extensive vascularization.

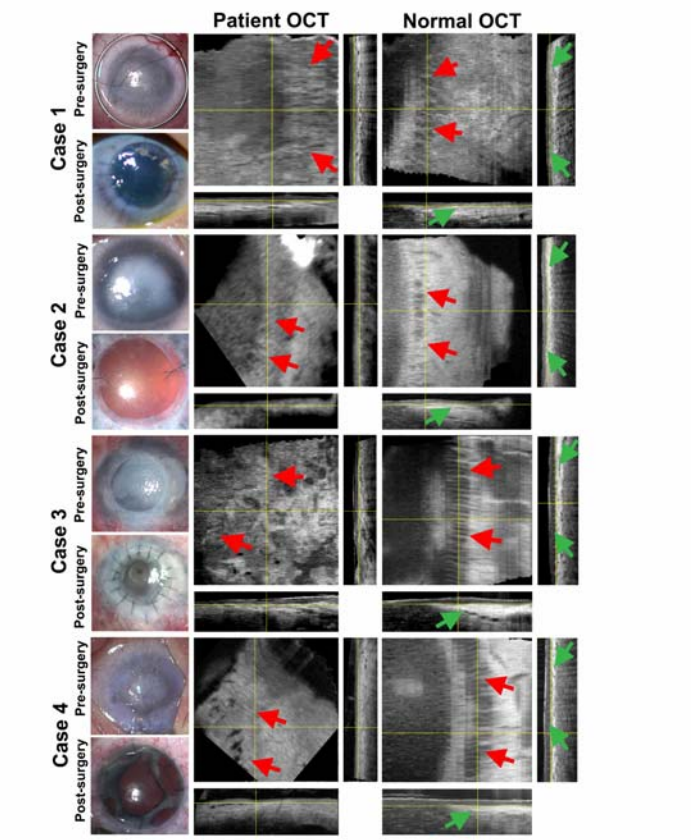

FIGURE 3

Examination results for cases 1, 2, 3, and 4. In all cases the cornea is oriented toward the left in the OCT images. Each trio of OCT images is displayed so that z plane is upper left, x plane is upper right, and y plane is lower left. Case 1, Preoperative image shows marked superficial vascularization with areas of heaped epithelium. Impression cytology was equivocal. Postkeratoplasty there is epithelialization with some punctate epithelial erosions but no peripheral neovascularization. At last follow-up (18 months) there were some peripheral new vessels and mild haze. OCT shows palisades that are not as prominent as those seen in the age-matched normal (red arrows). In x plane blood vessels are seen at the bases of ridges (not labeled), but similar vessels seen in the age-matched normal control are labeled with green arrows.

Case 2, Preoperative image shows an eccentric opacity due to kerato-irido-lenticular adhesion (Peters' anomaly type 1). Postoperatively the epithelium of the graft remains healed. There is no peripheral neovascularization and no staining. SD-OCT imaging of this patient shows rippling due to the palisade ridges (red arrows) in the enface z plane, which are not as prominent as those found in the age-matched normal. Blood vessels are seen at the base of ridges on x plane but are not as regular or consistent as those seen in the age-matched normal control (green arrows). The y-plane scans do not show vessels (green arrow) for the control, but on the dynamic scan they are seen.

Case 3, Patient had been born with corneal opacities and glaucoma and had previously undergone surgery with corneal graft. Preoperative image shows rejected graft and following re-transplant. Retinal detachment surgery had been performed simultaneously with the regraft, and silicone oil had been placed in the eye. A globule of silicone oil up against the epithelium is visible, but no neovascularization is seen at 8 months post graft. Enface OCT image shows sparse palisade ridges (red arrows), and blood vessels at base of the ridges are clearly seen on the x and y planes. These can be compared to those seen in the age-matched normal control (green arrows).

Case 4, Presurgical image shows bilateral congenital opacities with scleralization and vascularization, which were present in both eyes. The patient could follow light only with either eye. Right graft was performed later, and postsurgical image shows clear cornea with intact epithelium. Enface OCT in z plane shows the ripples of the palisade ridges (red arrows). Blood vessels seen at the base of the palisade ridges are seen in the x and y planes but are not as clear as those seen in the age-matched normal control (green arrows). These ridges, while present, are not completely normal when compared to the age-matched normal.

Case 5 (Figure 4)

A 13-month old boy with a history of congenital glaucoma following left trabeculectomy, right cyclophotocoagulation twice, and corneal opacities right worse than left, was referred from Hong Kong for a second opinion. Family history was not significant. On EUA, at induction, the IOP was 14 mm Hg in the right eye and 12 mm Hg in the left eye. Horizontal corneal diameter was 12.5 mm in the right eye and 9 mm in the left eye. There was a 360° pannus with avascular corneal opacity in the right eye. In the left eye there was a central corneal opacity with marked iridocorneal adhesions. B-scan of the right eye showed no keratolenticular adhesions, but there was a cataract present, with axial length of 24 mm. In the left eye the anterior chamber was shallow with a large lens and axial length of 19.5 mm. Electrodiagnostic testing revealed flash VEP within normal limits for age in both eyes, with smaller amplitude in the left eye. The patient underwent PKP with lensectomy and vitrectomy in the right eye and inferior broad iridectomy in the left eye.

The postoperative course was complicated by glaucoma in the right eye, which needed cyclophotocoagulation and Ahmed glaucoma tube implant. The patient developed cataract in the left eye, for which lensectomy was performed. At the last follow-up, 12 months after the right PKP, he was able to fix and follow the light with both eyes. Right eye cornea showed partial endothelial rejection of the graft. The Ahmed tube was in situ. In the left eye the cornea was clear in the superior half. Fundus examination of both eyes was within normal limits.

Histology showed keratinization of the corneal epithelium, extensive loss of Bowman's layer, condensation of posterior stroma with adherent pigment epithelium, and a partially discontinuous Descemet's membrane.

Case 6 (Figure 4)

A newborn full-term baby girl was delivered by C-section because of increased head circumference (99th percentile, 40 cm) and ventriculomegaly diagnosed prenatally. On systemic evaluation she was noted to have multiple congenital anomalies. Ocular examination revealed bilateral response to light. On EUA she was found to have bilateral microcorneas (HCD, 7 mm), axial lengths of 21.3 mm in the right eye and 23.2 mm in the left eye, bilateral aniridia, and a left hazy and edematous cornea. Pachymetry revealed central corneal thickness of 733 μm in the right eye and 1102 μm in the left eye. Fundus examination showed a dysplastic and cupped optic nerve in both eyes with a hazy view in the left eye due to corneal edema. Intraocular pressure with pneumotonometry was 23 mm Hg in the right eye and 33 mm Hg in the left eye. With these clinical findings a diagnosis of congenital glaucoma, aniridia, and microcornea was made. Molecular testing showed *normal* PAX6 alleles, suggesting that the LSCD associated with PAX6-related aniridia was unlikely to be present. She underwent multiple surgical procedures, including trabeculectomy, trabeculectomy with mitomycin-C, and cyclophotocoagulation in both eyes to control the pressures. Intraocular pressure was controlled in the right eye with some haziness of the nasal cornea. Despite the glaucoma surgeries and maximum medical treatment, the left eye showed persistent corneal opacity, uncontrolled IOP, and keratolenticular touch. She developed cataract in both eyes and underwent lensectomy in the right eye.

The patient subsequently developed a spontaneous perforation of the left cornea with the eye ultimately becoming phthisical secondary to postoperative endophthalmitis. Electrodiagnostic testing revealed flash VEP within normal limits for age in the right eye. Despite encouragement to avoid intervention, the parents were desperate to try to improve visual function in the right eye. After informed consent from the parents was obtained, the child underwent PKP with anterior vitrectomy in the right eye.

Postoperatively the epithelium would not heal in the lower four-fifths of the cornea. At the last follow-up, 10 months after the right PKP, the child (aged 2 years) blinked to light. Cornea was hazy in the right eye with scarring and vascularization. Histology of the corneal button showed keratinization and acanthosis of the corneal epithelium, calcific band keratopathy with multifocal breaks in Bowman's layer, extensive superficial stromal scarring, mild chronic keratitis (with negative staining for bacterial and fungal microorganisms), and paucity of corneal endothelial cells.

Case 7 (Figure 5)

A 12-month-old boy was referred on account of glaucoma and cloudy corneas in both eyes for 3 months. On examination, the child blinked to light and had central steady fixation and maintained fixation in both eyes. The corneas were mildly hazy with IOP of 10 mm Hg using rebound tonometry in both eyes. Corneal diameters were not increased and the cup-disc ratio was 0.1 to 0.2 in both eyes. Pachymetry revealed a corneal thickness of 1100 μm in either eye.

Eight weeks after the initial visit an EUA was performed. At induction IOP was found to be 9 mm Hg in either eye with Perkins tonometer. Horizontal corneal diameter was 10.5 mm in either eye. Axial length was 19.95 mm in the right eye and 19.87 mm in the left eye. Corneal thickness was 1166 μm in the right eye and 1152 μm in the left eye. The child had clear evidence of epithelial edema. The refraction was -2.5 in either eye. Fundus view was hazy with a cup-disc ratio of 0.1 in either eye. Ultrasound biomicroscopy showed a normal anterior chamber, but the echoes from the inner layer of the cornea (ie, the endothelium/Descemet's membrane complex) were abnormal. This was confirmed on handheld OCT, whereby subepithelial edema could be seen in the anterior third of the cornea and there appeared to be areas of the endothelial/Descemet's complex that were irregular or missing. The differential diagnoses were congenital hereditary endothelial dystrophy, posterior polymorphous dystrophy, and X-linked endothelial corneal dystrophy.

A second EUA was performed 9 months after initial presentation. At induction IOPs were 14 mm Hg in either eye. Horizontal corneal diameter was 11 mm in either eye. The cornea looked edematous with stromal edema, and retroillumination clearly showed endothelial changes. Both lenses were clear. Fundus was healthy with a cup-disc ratio of 0.0. The handheld OCT showed endothelial changes with stromal edema. The pachymetry showed corneal thickness to be 1061 μm in the right eye and 1056 μm in the left eye. Axial length was 21.48 mm in the right eye and 21.14 mm in the left. The refraction was -3.00 D in the right eye and -2.00 D in the left. Electrodiagnostic testing revealed normal flash and pattern VEP.

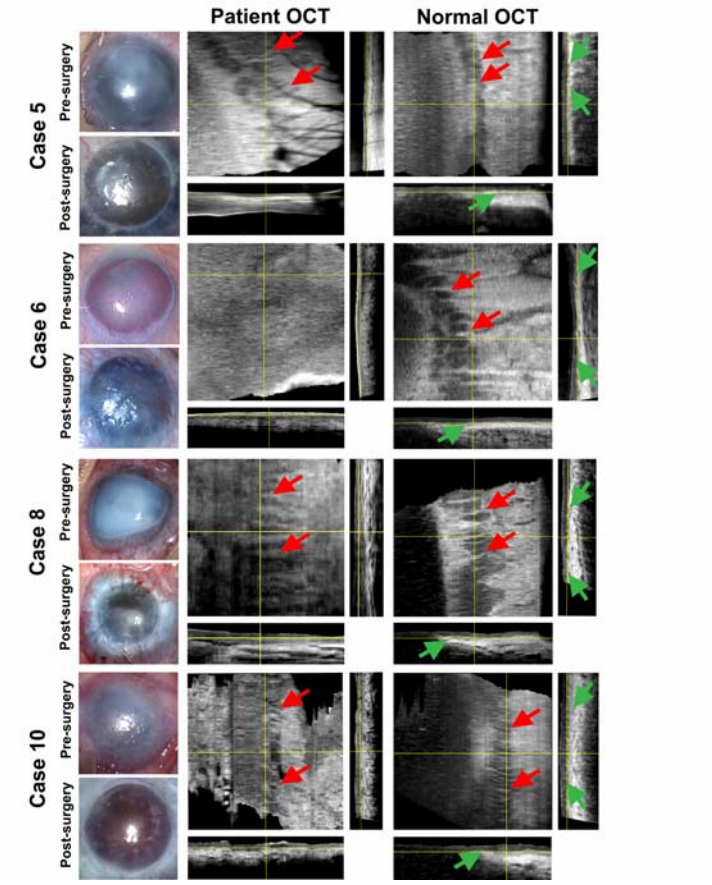

FIGURE 4

Examination results for cases 5, 6, 8, and 10. In all cases the cornea is oriented toward the left in the OCT images. Each trio of OCT images is displayed so that the z plane is upper left, x plane is upper right, and y plane is lower left. Case 5, Patient had a corneal opacity that has superficial vessels in one quadrant. Preoperative image shows that the central opacity is avascular and that there is 360° pannus that stops abruptly, similar to but not as dramatic as that seen in case 8. Postcorneal graft shows neovascularization for 120° with some epithelial defects but epithelialization is present. Evaluation of the OCT video stack of z plane did not show ridges consistently, but the image shown here presents the best image of the ridges possible (red arrows). Blood vessels are seen but are not consistent (x plane) compared to those seen in the age-matched control (green arrows).

Case 6, Patient had congenital corneal opacities. Left eye developed a spontaneous corneal perforation and was lost. After repeated requests from the parents, consideration was given to corneal grafting of the right eye. The usual signs of limbal stem cell absence or deficiency (conjunctivalization, neovascularization, and chronic inflammation) were not seen (presurgical image) and the decision was made to graft. Post surgery there was failure of normal epithelialization and eventual opacification of the graft with only a small area of clarity remaining. OCT evaluation failed to show any signs of palisade ridges or the blood vessels at the base of the ridges. Compare to the age-matched normal with palisade structures marked (red arrows).

Case 8, Patient had unilateral corneal opacity and bilateral glaucoma. Patient compliance with corneal graft follow-up was poor, and an infectious keratitis developed, the residual haze of which is evident (postsurgery). The epithelium healed and there is no peripheral vascularization. Preoperative image shows a very clear delineation of the peripheral scleralization and the start of the opaque cornea with no keratolenticular adhesion. OCT evaluation shows clear palisade ripples (red arrows), and the blood vessels at their bases are very clearly seen in x and y planes. They are comparable to those seen in the age-matched normal control (green arrows).

Case 10, Patient had Axenfeld-Rieger anomaly with glaucoma. Cataract surgery had been performed previously, and the cornea had become more cloudy after the extraction. At 13 months follow-up the epithelium had healed but retinal detachment developed. OCT evaluation was conducted successfully with the patient awake despite the nystagmus. Some motion artifact is clear in the z plane but does not interfere with the determination of palisades. Blood vessels at the bases of the ridges are present.

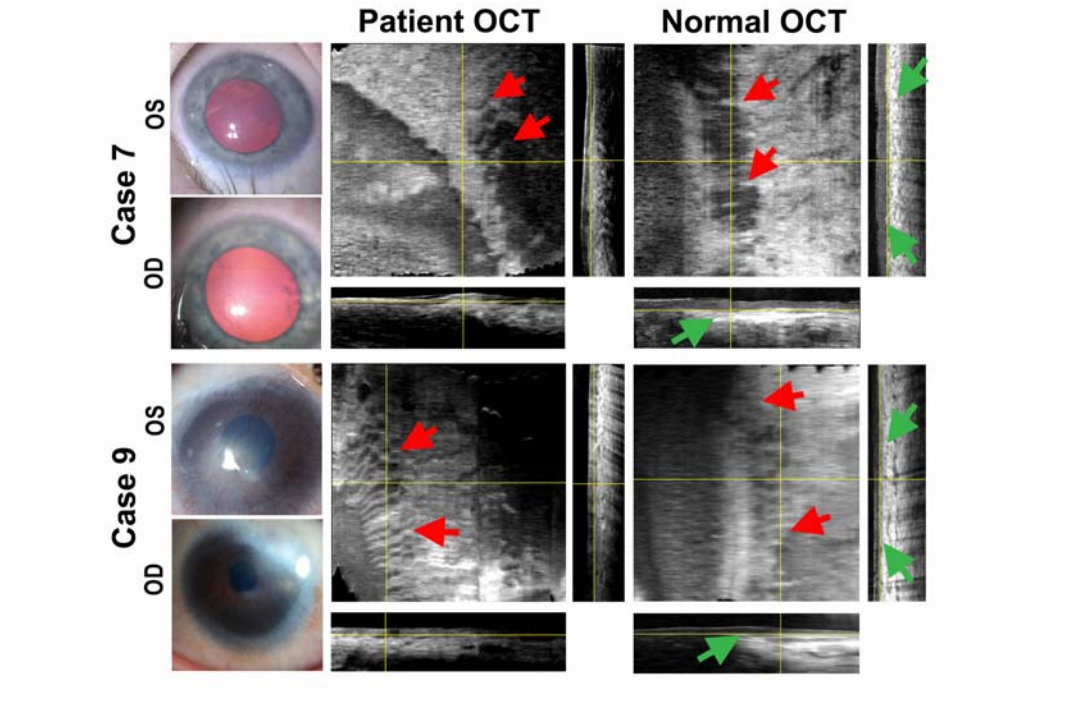

FIGURE 5

Examination results for cases 7 and 9. In all cases the cornea is oriented toward the left in the OCT images. Each trio of OCT images is displayed so that the z plane is upper left, x plane is upper right, and y plane is lower left. Neither case went on to have penetrating keratoplasty. Case 7, Patient has signs of an endothelial dystrophy. Molecular genetic testing is awaited. The corneal epithelium is clear and normal. The patient has not had surgical intervention yet. OCT evaluation reveals palisade ridges on the enface z plane (red arrows) and the blood vessels at their bases in the x and y planes.

Case 9, Patient has had bilateral scleralization with corneal vascularization since birth. Corneas are relatively flat and nystagmus is present. She is not scheduled for corneal transplant. OCT evaluation was conducted successfully despite the nystagmus, although some motion artifact is evident in z plane. The palisade ridges are clearly present, and the blood vessels at the base of the ridges are also visible.

Case 8 (Figure 4)

A 2-year-old Asian girl, adopted soon after birth and with a history of glaucoma in both eyes and corneal opacity in the left eye, was referred for further evaluation. She had had glaucoma surgeries, including an Ahmed drainage device in both eyes and goniotomy in both eyes, 4 weeks before she presented to us. At EUA, during induction phase, IOP was at 13 mm Hg in the right eye and 14 mm Hg in the left eye using a pneumotonometer. The HCDs were 12 mm in the right eye and 11 mm in the left eye. Examination of the anterior segment of the right eye revealed a clear cornea, except for one area of discrete opacity at the tip of the Ahmed tube; however, there was no corneal touch of the tube to the cornea at that location. The lens was clear. Fundus examination showed a cup-disc ratio of 0.1 mm with a healthy-appearing optic nerve with normal macula and peripheral retina. Refraction of the right eye measured -7.00, -1.00 at 180°.

The left eye showed a diffusely cloudy cornea with an irregular shape. Scleralization seen peripherally stopped abruptly at a distinct line. A tube shunt superotemporally was well covered with surrounding adjacent diffuse bleb. There was no view into the anterior chamber or posterior pole, and no refraction was possible.

On EUA 3 months later, IOP was 22 mm Hg in the right eye and 32 mm Hg in the left eye. Corneal diameter was 13.5 mm in the right eye and 12 mm in the left eye. Flushing and trimming of the right eye drainage tube was performed. On subsequent follow-up, 6 months after the initial presentation, the patient's IOP was controlled in both eyes with persistence of corneal opacity in the left eye. Electrodiagnostic testing revealed flash VEP within normal limits for age in both eyes. After informed consent from the parents was obtained, the patient underwent PKP in the left eye. Eight weeks postoperatively she developed an infective corneal ulcer in the left eye, which led to the rejection of the graft. She underwent another PKP with lensectomy and vitrectomy in the left eye, as ultrasound

biomicroscopy before PKP revealed the presence of cataract.

At the last follow-up, 4 months after the second PKP, her visual acuity was 20/100. Horizontal corneal diameter was 13 mm in the right eye and 11 mm in the left eye. The cornea of the right side was clear except for a little bit of punctate epithelial erosions inferiorly. The cornea of the left eye showed an epithelial defect centrally, and the corneal graft appeared edematous. Intraocular pressure was normal digitally in both eyes. Fundus examination of the right eye showed a cup-disc ratio of 0.2, and the refraction in the right eye was -5 with +3.5 at 15°. B-scan showed normal posterior segment in both eyes. At last follow-up the child had partial clarity of her graft.

Histology of the corneal button showed keratinizing and acanthotic corneal epithelium with chronic keratitis and increased melanocytes in the superficial stroma with dense, disorganized collagen structure. There was near complete absence of Bowman's layer, absence of Descemet's membrane centrally, a paucity of corneal endothelial cells, and a central stroma with mucoid degeneration. Melanocytes were also noted in the central corneal epithelium. No microbial organisms were seen on periodic acid–Schiff stain.

Case 9 (Figure 5)

A 14-year-old girl presented with bilateral cloudy corneas. She had a history of trabeculectomies and a repair of intrastromal bleb performed elsewhere. Unaided visual acuity for distance was 20/300 OD and 20/200 OS. Her near visual acuity was 20/70 OD and 20/40 OS, and she had jerk latent nystagmus. Intraocular pressure was 10 mm Hg in the right eye and 8 mm Hg in the left eye with applanation tonometry. Digitally the pressure was higher in both eyes. The corneal pachymetry was 559 μm in the right eye and 597 μm in the left. Her corneas clinically appeared flat; keratometry could not be completed successfully.

On slit-lamp examination, the cornea showed central opacity with vascularization in both eyes, the right eye worse than the left. The anterior chamber was shallow in both eyes. Lens was clear in either eye with a capsular bag diameter of approximately 10 mm. Fundus examination revealed a cup-disc ratio of 0.5 with loss of temporal neuroretinal rim in the right eye and a cup-disc ratio of 0.2 in the left eye. A tentative diagnosis of cornea plana was made. After dilation, IOP dropped to 6 mm Hg in the right eye and there was no change in the left eye. The anterior chambers also deepened after dilation.

Case 10 (Figure 4)

A 4-year-old boy was referred for a second opinion. He was known to have molecularly confirmed bilateral Axenfeld-Rieger syndrome and glaucoma with a FOXC1 mutation. He had Baerveldt implants in both eyes and PKP in the left eye.

On ocular evaluation his best-corrected visual acuity (BCVA) was counting fingers at 3 feet with -4.75 D OD and light perception with -4.50 D OS. Intraocular pressure was 11 mg in the right eye and moderate on digital tonometry in the left eye. On slit-lamp evaluation the right cornea was hazy with a tube-endothelial touch superotemporally. He was noted to have corectopia. The corneal haze precluded retinoscopy and detailed fundus examination. Left eye showed corneal opacity secondary to failed graft. The view of the anterior chamber was hazy.

On EUA, the IOP at induction was 4 mm Hg in the right eye and 18 mm Hg in the left eye. Horizontal corneal diameters were 9.5 mm in the right eye and 7.5 mm in the left eye. The left cornea had a central scarred area. B-scan clearly showed keratolenticular lesion in this area with a normal posterior segment. In the right eye there was opacity in the upper two-fifths of the cornea, where the drainage tube was touching the endothelium. B-scan revealed a normal posterior segment in the right eye. The patient underwent right drainage tube shortening and flushing, lysis, and division of extensive posterior pigment epithelium attachments to the anterior capsule and broad iridectomy in the right eye. Postoperatively he received topical corticosteroids and topical antiglaucoma medications. Subsequently he underwent PKP with lensectomy and anterior vitrectomy in the left eye. The patient followed up locally, where he underwent cataract extraction in the right eye. At the next follow-up visit with us, 17 months after the left PKP, his BCVA was hand movements with +18.00 D OD and counting fingers close to the face with +12.00 D OS. Slit-lamp examination revealed corneal opacity with pannus and vascularization in the superior half in the right eye. The anterior chamber and iris were normal with aphakia. The left eye showed a failed corneal graft. He underwent PKP with vitrectomy and membranectomy in the right eye.

The patient's postoperative course was complicated by retrocorneal membrane with fibrovascular tissue and inferior tractional retinal detachment. After much counseling, he received intravitreal bevacizumab. At the last follow-up, 9 months after the right PKP, his BCVA was 20/400 OD for near and light perception OS. There was a tractional retinal detachment inferiorly. Intraocular pressure was normal in both eyes. The corneal epithelium healed with no new epithelial vascularization. Histopathology of the right corneal button revealed keratinization of the corneal epithelium, stromal scarring with absence of Bowman's layer, focal chronic inflammation of the corneal epithelium and stroma, and vascularization of the corneal stroma. There was duplication of Descemet's membrane with focal plaque formation.

ANALYSIS OF OCT IMAGES

Volumes were acquired at the limbus and analyzed in three dimensions (see Figures 3, 4, and 5). For the sake of this manuscript the three planes are shown as static images, but videos of all the stacks of images were reviewed, as this gives a better understanding of the information available. (Similarly, dynamic ultrasound B-scan is preferable to assess the presence of a retinal detachment, but often static scans are used to demonstrate the presence or absence of a retinal detachment.)

Normal volumes were acquired from age-matched subjects who had no known corneal problems in the eye examined. Scans were reconstructed to show the x, y, and z planes, with particular attention drawn to not only the POV ridges but also the blood vessels at their bases. The scans were analyzed by one observer (K.L.L.), who was masked to the clinician's (K.K.N.) assessment of the ocular

surface with respect to clinical signs of LSCD. The superior and inferior limbus was preferentially scanned. The presence of "rippling" seen on a video of the stacks of images and the presence of blood vessels were enough for the presence of POV to be considered. On the static z-plane images the presence of ridges was evaluated and characterized as regular or irregular. On the x-plane image the presence of ridges was again evaluated and the presence of blood vessels at the base of the ridges was also assessed.

Impression cytology was not performed except in one case, but it is our experience that in eyes with CCO, impression cytology rarely yields any useful information (unpublished data: three eyes of neonatal corneal opacification with insufficient sampling despite using regular impression cytology techniques).

RESULTS

All patients were successfully scanned with no adverse events (see Figures 3, 4, and 5).

All control eyes showed the presence of POV, but the regularity and uniformity of ridges and blood vessels, especially in the x-plane view, varied (see Table 6). Eyes under the age of 18 months displayed the least consistent ridges on the z-plane view and variable blood vessels on the x-plane view (see Table 6, control figures for cases 2, 4, and 7: note case 7 control is 14 months old and cases 2 and 4 controls are 1 month old). The older the control, the more consistent the ridges and the blood vessels (see Table 6, controls for cases 1, 3, 9, and 10). For the sake of clarity, normal POV are expected to show uniform and regular ridges on the z-plane view and ridges with blood vessels at the bases of the ridges on the x-plane view. The y-plane view is useful for confirming the position of the limbus and showing the vessels rising through the connective tissue to the base of the palisades. This view is best appreciated as an image sequence rendered as a movie.

Two patients (cases 9 and 10) were scanned while awake; both had nystagmus, but despite this, volumes of sufficient detail were acquired. An artifact was seen in both cases caused by the saccadic component of a jerk nystagmus (see Figures 4 and 5), but signs of POV were found. In case 9 both eyes were determined to have presence of POV; palisade ridges were seen regularly but were not uniform, and blood vessels were seen on x-plane view (Figure 5). In case 10 POV were observed in the right eye; palisade ridges were seen but were not uniform, and although blood vessels were seen, they were sparse (Figure 4). Corneal transplant was performed, and at 11 months post transplant the epithelium had healed and showed no signs of peripheral epithelial vascularization or unusual whorl-like staining pattern with fluorescein (Figure 4).

Four children under the age of 18 months were examined (cases 2, 4, 5, and 7). Case 2 had an opacity that was avascular but had keratolenticular adhesion with iridocorneal adhesion. This case showed evidence of POV; ridges were present but not regular or uniform, and while blood vessels were seen on x-plane view, clear ridges were not (see Figure 3). This child went on to have a PKP. The epithelium remained intact with no peripheral vascularization (Figure 3). Case 4 had bilateral PKP. The OCT demonstrated presence of POV; the right eye showed regular, uniform ridges with ridges also seen with blood vessels on the x-plane view, whereas the left eye showed irregular and nonuniform ridges on z-plane view and blood vessels but no ridges on x-plane view (see Figure 3: only SD-OCT of left eye is shown in this figure). In this child the left PKP developed stromal vessels and endothelial failure, but the epithelium remained intact with no staining. The right graft remains clear with no new vessels. Case 5 had a corneal opacity in the right eye. POV were seen on OCT with ridges that were regular if not uniform, and ridges and blood vessels were seen on x-plane view (see Figure 4). This eye underwent PKP and the epithelium healed slowly; it is difficult to know whether this was due to uncontrolled glaucoma or abnormal epithelial healing. While there was haze at last follow-up, the epithelium had healed with some subepithelial haze but no peripheral corneal vascularization. Case 7 has an endothelial dystrophy with a normal limbus, which is borne out by the OCT identifying POV. While the ridges were present and regular, they were not uniform, although ridges and blood vessels were seen on x-plane view (see Figure 5).

Two patients (cases 6 and 8) were under 3 years but over 18 months at examination. Case 6 was the only case where no POV could be seen (see Figure 4). Since the opacity in this girl's case was not vascularized, the decision to perform a PKP had been made, and the procedure resulted in a persistent defect for about two-thirds of the cornea with an eventual scar in this area extending to four-fifths of the cornea. Case 8 had compliance issues and developed an infectious keratitis, but the appearance of the opacity preoperatively was rather unusual with a heaped opacity with vascularization. Clinically it was difficult to know if there was LSCD. The OCT demonstrated POV that were uniform but not regular, and blood vessels were seen on the x- and y-plane views. Following keratoplasty the epithelium healed immediately.

In case 3 the OCT demonstrated POV in the left eye with ridges that were present and uniform but not regular, with blood vessels seen on the x- and y-plane views but no clear ridges seen on the x-plane view (see Figure 3). While the corneal graft developed complications as a result of silicone oil in the eye, the epithelium healed adequately and showed no vascularization.

Case 1 showed bilateral corneal vascularization and had clinically been previously diagnosed with LSCD. The OCT revealed evidence of POV with ridges that were present although not uniform or regular but with very good vasculature at the base of the palisade ridges on the x-plane view (see Figure 3). While corneal grafts show clear central axes, the peripheral corneas show some opacity. There was endothelial graft rejection in both eyes, and the epithelium remained intact but not clear to the periphery in both eyes.

DISCUSSION

Ten cases in this series with CCO and 10 normal age-matched eyes underwent SD-OCT evaluation. One of the affected eyes (case 3) had a previous corneal transplantation performed elsewhere, which had failed. Regraft was performed in part to help manage posterior

segment disease. Nevertheless, the original etiology was congenital corneal opacity. Since there is no evidence that the donor cornea can induce any POV microenvironment where none was present in the host limbus previously, assessment of the POV in this patient was included to help evaluate the case.

To the best of our knowledge, no previous studies have been performed on the POV of children with congenital corneal opacities. While this study does not present a comprehensive evaluation of pediatric POV or of POV status of all types of CCO, it does describe the POV in children with CCO and age-matched normals. Congenital corneal opacification is a very rare condition, which explains the small numbers in this study. The lack of impression cytology in this study may be considered a weakness; however, no such previous studies have been performed, and this may be because the routine impression cytology techniques may not remove sufficient cells to make an evaluation viable. The presence of keratinized epithelium in almost all the histological corneal buttons studied supports this assessment. Other factors influencing the ocular microenvironment and ultimate survival of the graft, such as corneal wetting, tear film, corneal sensation, exposure keratopathy, and conjunctival mucin production, have not been evaluated in this study. Despite POV being present in the majority of cases to a varying degree, the clarity of the graft was still dependent on endothelial function, control of glaucoma, and posterior segment disease. The secondary aim of this study was not to evaluate graft survival but to evaluate only postkeratoplasty epithelialization.

This study makes the assumption that the presence of POV is a requirement for functioning limbal stem cells. While the evidence in the literature strongly suggests that this is the case, we have not in this study directly visualized the limbal stem cells.

We found that the younger the control eye, the less likely the regularity and consistency of the palisade ridges. In controls 2, 4, and 7, the ridges are not nearly as regular as those seen in older control eyes (eg, 1, 3, and 10).

Congenital corneal opacification is rare, but our center attracts patients nationally and internationally and we have a dedicated evaluation and treatment protocol (Figure 6). The etiology of CCO varies but is best evaluated in terms of primary or secondary corneal disease.[3,4] Both may be developmental or may be acquired with secondary causes (see Table 1). There is, to the best of our knowledge, no information about the status of the POV or limbal stem cells in CCO.

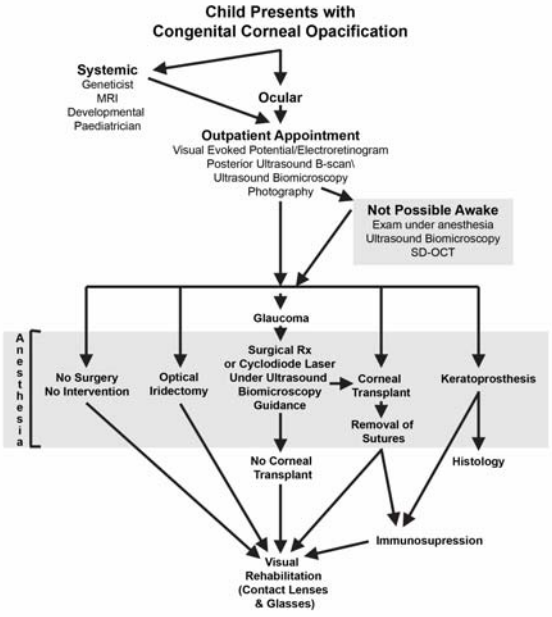

FIGURE 6

Evaluation protocol and treatment algorithm for neonatal corneal opacification. Note that a systemic evaluation is very important with genetic evaluation, neuroimaging, and general pediatric review. Ocular examination must include both anatomical (USS) and functional (VEP/ERG) evaluation of the posterior segment. Any glaucoma that is present must be treated before any other intervention is considered. While keratoprosthesis is included here, it is usually considered only after multiple failed grafts.

While there is much published about the outcomes of corneal transplantation in CCO, perusal of the relevant literature fails to define the nature of corneal graft failure.[5-25] Retrocorneal membranes have been implicated in cases of aphakia but not specifically in

children. The success of corneal transplantation depends on adequate replenishment of the epithelium, maintenance of stromal clarity with no stromal new vessels, and maintenance of the endothelial pump. This study, to the best of our knowledge, is the first to address the issue of palisade structure and variation in congenital corneal opacities.

Although POV can sometimes be evaluated clinically using a slit lamp,[43,44] this is not so easily or reliably done for neonates, infants, or toddlers. It is also not possible for children with nystagmus or for patients under anesthesia to be evaluated with only a handheld slit lamp. While confocal microscopy has been used successfully to image the POV,[40,41] it has a very small field of view, which prohibits evaluation of large areas of the limbus, and it is a contact technology requiring the patient to sit upright, precluding its use in pediatric populations.

We specifically looked at the superior and inferior limbus because the POV are found in these regions more often and with greater density.[43] We looked for uniform and regular palisade ridges as well as blood vessels at the base of the ridges of the palisades. Recent work has shown that the limbal microvasculature is extremely important in the maintenance of limbal stem cells.[45]

The triad of conjunctivalization, corneal neovascularization, and chronic inflammation is not pathognomonic of LSCD, and several studies have impressed upon the false-positive diagnosis of LSCD when relying only on clinical features.[40] Impression cytology looking for goblet cells on the cornea and specific epithelial keratin and mucin markers for corneal or conjunctival epithelium has been well described, with the exact keratin or mucin determination varying from group to group.[36-39] This method relies on the use of a cellulose membrane being applied to the corneal and conjunctival surface and then removed, peeling away superficial epithelial cells and goblet cells. Normal corneal epithelium is nonkeratinized and stratified. However, it is our experience that adequate sampling is not usually achieved, and one explanation might be that the histology of the cases undergoing PKP often shows keratinization of the corneal epithelium. Nevertheless, since most children would need to be anesthetized or sedated to do such an evaluation, the likely low yield of results makes impression cytology less favorable for children with CCO.

None of the histological specimens from these cases showed goblet cells, which have been shown in keratopathy secondary to PAX6-related aniridia.[32] The fact that loss of POV in an area previously known to have them (usually after alkali injury or Stevens-Johnson syndrome), or the loss of POV architecture in aniridic keratopathy, is associated with clinical features of LSCD suggests that the POV are a sign of normally functioning limbal stem cells.[26,30,32]

We found that only two eyes of the cases examined demonstrated robust POV (palisade ridges present in all three planes in a pattern and density comparable to the normal eyes scanned, with vasculature at the base of each palisade ridge); seven eyes showed varying degrees of POV, and in the only eye where POV were not demonstrated at all, the failure of the graft was due to persistent epithelial deficit with heaping of the epithelium and opacification on the graft at the epithelial and subepithelial level. In all the other cases where the POV were visible to varying extents, the epithelium appeared to heal. While an argument can be made that the follow-up of all the cases was not beyond a year, in all cases previously published in which there has been LSCD[26] or where in experimental animal models LSCD has been created,[27] the peripheral cornea becomes vascularized. In case 1, where this has happened, there were mild vessels and the follow-up was beyond a year. In other cases where retrocorneal membranes formed or there was endothelial rejection, the epithelium remained clear both centrally and in the periphery.

This study shows not only that in cases of CCO the POV may be present but not entirely normal, but also that while the clinical signs of LSCD may be present (cases 1, 4, and 9), POV may still be seen. In all these cases where PKP was done and some degree of POV identified, epithelialization occurred. Interestingly, in the one case (case 6) where no POV were seen on OCT, clinically none of the classic triad of LSCD was present and the epithelium failed to heal at all. It is worth noting that although this patient had aniridia, her molecular diagnosis failed to reveal any mutations in *PAX6*, *FOXC1*, or *PITX2* (the three genes most commonly associated with aniridia). Furthermore, only PAX6-related aniridia is associated with LSCD, and the patient was negative for this.

CONCLUSION

We have demonstrated that OCT is capable of imaging POV in children, and that most children with congenital corneal opacity have identifiable POV compared to age-matched normals. These POV may be completely present or partially present. In each case where they were present and where PKP was performed, epithelialization was seen following transplant. In all cases where follow-up was beyond 1 year, central epithelialization was still present. In the only case where there was no evidence of POV, there was failure of epithelialization following transplant.

ACKNOWLEDGMENTS

Funding/Support: This work was supported by Core Grant for Vision Research EY-08098 and by the Pfeiffer Foundation.

Financial Disclosures: Dr Nischal has received a fee as a one-off advisor to Bausch and Lomb in December 2015 and has received an Honorarium from Clarity Inc for a lecture in 2013.

Author Contributions: Design and conduct of the study (K.K.N., K.L.L.); Collection of data (K.K.N., K.L.L.); Analysis (K.K.N., K.L.L.) and interpretation (K.K.N., K.L.L.) of the data; Preparation of manuscript (K.K.N., K.L.L.); Review (K.K.N., K.L.L.) and approval (K.K.N.) of manuscript.

Other Acknowledgments: The authors thank Jessica Steele for assistance in image processing and analysis and T. Tobiassen and Students for Sustainable Medical Development for assistance in developing the mount.

REFERENCES

1. Bermejo E, Martinez-Frias ML. Congenital eye malformations: clinical epidemiological analysis of 1,124,654 consecutive births in Spain. *Am J Med Genet* 1998;75:497-504.
2. Kurilec JM, Zaidman GW. Incidence of Peters anomaly and congenital corneal opacities interfering with vision in the United States. *Cornea* 2014;33(8):848-850.
3. Nischal KK. A new approach to the classification of neonatal corneal opacities. *Curr Opin Ophthalmol* 2012;23(5):344-345.
4. Nischal KK. Congenital corneal opacities: a surgical approach to nomenclature and classification. *Eye* (Lond) 2007;21(10):1326-1337.
5. Chang JW, Kim MK, Kim JH, Kim SJ, Wee WR, Yu YS. Long-term visual outcomes of penetrating keratoplasty for Peters anomaly. *Graefes Arch Clin Exp Ophthalmol* 2013;251(3):953-958.
6. Limaiem R, Chebil A, Baba A, Ben Youssef N, Mghaieth F, El Matri L. Pediatric penetrating keratoplasty: indications and outcomes. *Transplant Pro.* 2011;43(2):649-651.
7. Huang C, O'Hara M, Mannis MJ. Primary pediatric keratoplasty: indications and outcomes. *Cornea* 2009;28(9):1003-1008.
8. Vanathi M, Panda A, Vengayil S, Chaudhuri Z, Dada T. Pediatric keratoplasty. *Surv Ophthalmol* 2009;54(2):245-271.
9. Rao KV, Fernandes M, Gangopadhyay N, Vemuganti GK, Krishnaiah S, Sangwan VS. Outcome of penetrating keratoplasty for Peters anomaly. *Cornea* 2008;27(7):749-753.
10. Ricci B, Coppola G, Capobianco A, Ziccardi L. Penetrating keratoplasty in a newborn: case report and analysis of current surgical trends in Italy. *Eur J Ophthalmol* 2008;18(2):290-293.
11. Zaidman GW, Flanagan JK, Furey CC. Long-term visual prognosis in children after corneal transplant surgery for Peters anomaly type I. *Am J Ophthalmol* 2007;144(1):104-108.
12. Al-Ghamdi A, Al-Rajhi A, Wagoner MD. Primary pediatric keratoplasty: indications, graft survival, and visual outcome. *J AAPOS* 2007;11(1):41-47.
13. Michaeli A, Markovich A, Rootman DS. Corneal transplants for the treatment of congenital corneal opacities. *J Pediatr Ophthalmol Strabismus* 2005;42(1):34-44.
14. Yang LL, Lambert SR. Peters' anomaly. a synopsis of surgical management and visual outcome. *Ophthalmol Clin North Am* 2001;14(3):467-477.
15. Yang LL, Lambert SR, Lynn MJ, Stulting RD. Long-term results of corneal graft survival in infants and children with Peters anomaly. *Ophthalmology* 1999;106(4):833-848.
16. Frueh BE, Brown SI. Transplantation of congenitally opaque corneas. *Br J Ophthalmol* 1997;81(12):1064-1069.
17. Parmley VC, Stonecipher KG, Rowsey JJ. Peters' anomaly: a review of 26 penetrating keratoplasties in infants. *Ophthalmic Surg* 1993;24(1):31-35.
18. Comer RM, Daya SM, O'Keefe M. Penetrating keratoplasty in infants. *J AAPOS* 2001;5(5):285-290.
19. Frueh BE, Brown SI. Transplantation of congenitally opaque corneas. *Br J Ophthalmol* 1997;81(12):1064-1069.
20. Dana MR, Schaumberg DA, Moyes AL, Gomes JA. Corneal transplantation in children with Peter's anomaly and mesenchymal dysgenesis. Multicenter Pediatric Keratoplasty Study. *Ophthalmology* 1997;104(10):1580-1586.
21. Dana MR, Moyes AL, Gomes JA, et al. The indications for and outcome in pediatric keratoplasty. A multicenter study. *Ophthalmology* 1995;102(8):1129-1138.
22. Lowe MT, Keane MC, Coster DJ, et al. The outcome of corneal transplantation in infants, children, and adolescents. *Ophthalmology* 2011;118(3): 492-497.
23. Bhandari R, Ferri S, Whittaker B, Liu M, Lazzaro DR. Peters anomaly: review of the literature. *Corne.* 2011;30(8):939-944.
24. Patel HY, Ormonde S, Brookes NH, Moffatt LS, McGhee CN. The indications and outcome of paediatric corneal transplantation in New Zealand: 1991-2003. *Br J Ophthalmol* 2005;89(4):404-408.
25. Seitz B, Hager T, Szentmáry N, Langenbucher A, Naumann G. [Keratoplasty in children—still a dilemma]. *Klin Monatsbl Augenheilkd* 2013;230(6):587-594.
26. Dua HS, Azuara-Blanco A. Limbal stem cells of the corneal epithelium. *Surv Ophthalmo.* 2000;44(5):415-425.
27. Huang AJ, Tseng SC. Corneal epithelial wound healing in the absence of limbal epithelium. *Invest Ophthalmol Vis Sci* 1991;32(1):96-105.
28. Schermer A, Galvin S, Sun TT. Differentiation-related expression of a major 64K corneal keratin in vivo and in culture suggests limbal location of corneal epithelial stem cells. *J Cell Biol* 1986;103(1):49-62.
29. Chugh JP, Jain P, Sen R. Comparative analysis of fresh and dry preserved amniotic membrane transplantation in partial limbal stem cell deficiency. *Int Ophthalmol* 2015;35(3):347-355.
30. . Eberwein P, Reinhard T. Concise reviews: the role of biomechanics in the limbal stem cell niche: new insights for our understanding of this structure. Stem Cells 2015;33(3):916-924.
31. Lagali N, Edén U, Utheim TP, et al. In vivo morphology of the limbal palisades of Vogt correlates with progressive stem cell deficiency in aniridia-related keratopathy. *Invest Ophthalmol Vis Sci* 2013;54(8):5333-5342.
32. Kinoshita S, Friend J, Thoft RA. Sex chromatin of donor corneal epithelium in rabbits. *Invest Ophthalmol Vis Sci* 1981;21(3):434-441.
33. Nishida K, Kinoshita S, Ohashi Y, et al. Ocular surface abnormalities in aniridia. *Am J Ophthalmol* 1995;120:368-375.

34. Iorio E, Kaye S, Ponzin D, et al Limbal stem cell deficiency and ocular phenotype in ectrodactyly-ectodermal dysplasia clefting syndrome caused by p63 mutations. *Ophthalmology* 2012;119:74-83.
35. Garcia I, Etxebarria J, Merayo-Lloves J, et al. Novel molecular diagnostic system of limbal stem cell deficiency based on MUC5AC transcript deletion in corneal epithelium by PCR-reverse dot blot. *Invest Ophthalmol Vis Sci* 2013;54:5643-5652.
36. Mataftsi A, Islam L, Kelberman D, Sowden JC, Nischal KK. Chromosome abnormalities and the genetics of congenital corneal opacification. *Mol Vis* 2011;17:1624-1640.
37. Garcia I, Etxebarria J, Boto-de-Los-Bueis A, et al. Comparative study of limbal stem cell deficiency diagnosis methods: detection of MUC5AC mRNA and goblet cells in cornea epithelium. *Ophthalmology* 2012;119(5):923-929.
38. Paris Fdos S, Gonçalves ED, Barros Jde N, et al. Impression cytology findings in bullous keratopathy. *Br J Ophthalmol* 2010;94(6):773-776.
39. Di Iorio E, Ferrari S, Fasolo A, Böhm E, Ponzin D, Barbaro V. Techniques for culture and assessment of limbal stem cell grafts. *Ocul Surf* 2010;8(3):146-153.
40. Ramirez-Miranda A, Nakatsu MN, Zarei-Ghanavati S, et al. Keratin 13 is a more specific marker of conjunctival epithelium than keratin 19. *Mol Vis* 2011;17:1652-1661.
41. Nubile M, Lanzini M, Miri A, et al. In vivo confocal microscopy in diagnosis of limbal stem cell deficiency. *Am J Ophthalmol* 2013;155(2):220-232.
42. Miri A, Al-Aqaba M, Otri AM, et al. In vivo confocal microscopic features of normal limbus. *Br J Ophthalmol* 2012;96(4):530-536.
43. Lathrop KL, Gupta D, Kagemann L, Schuman JS, Sundarraj N. Optical coherence tomography as a rapid, accurate, noncontact method of visualizing the palisades of Vogt. *Invest Ophthalmol Vis Sci* 2012;53(3):1381-1387.
44. Goldberg M. In vivo confocal microscopy and diagnosis of limbal stem cell deficiency. Photographing the palisades of Vogt and limbal stem cells. *Am J Ophthalmol* 2013;156:205.
45. Takahashi N, Chikama T, Yanai R, Nishida T. Structures of the corneal limbus detected by laser-scanning confocal biomicroscopy as related to the palisades of Vogt detected by slit-lamp microscopy. *Jpn J Ophthalmol* 2009;53(3):199-203.
46. Huang M, Wang B, Wan P, et al. Roles of limbal microvascular net and limbal stroma in regulating maintenance of limbal epithelial stem cells. *Cell Tissue Res* 2015;359(2):547-563.
47. Kelberman D, Islam L, Jacques TS, et al. CYP1B1-related anterior segment developmental anomalies novel mutations for infantile glaucoma and von Hippel's ulcer revisited. *Ophthalmology* 2011;118(9):1865-1873.